International Journal of Thermophysics, Vol. 8, No. 5, 1987

Temperature and Pressure Effects on the Thermal Conductivity of TlCl and TlBr

R. J. Gummow[1] and I. Sigalas[1]

Received December 10, 1986

The hot-wire method was used to measure the thermal conductivity of both TlCl and TlBr. The measurements were performed in the temperature range 120–300 K and at pressures up to 2.3 GPa. An analysis of the thermal conductivity data showed that the Leibfried–Schlömann formula is a better description for TlBr than for TlCl. For both TlBr and TlCl the effect of optic phonons on thermal conductivity cannot be ignored.

KEY WORDS: high pressure; hot-wire method; thallium bromide (TlBr); thallium chloride (TlCl); thermal conductivity.

1. INTRODUCTION

The alkali halides are of special importance in the study of the thermal conductivity (λ) of crystals under pressure, because of the relatively simple crystal structures involved.

The temperature and pressure dependence of the thermal conductivity of many alkali halides has been investigated for both the NaCl and the CsCl crystal structures [1]. Attempts have also been made to find systematic trends among these materials [2].

Thallium chloride and thallium bromide both crystallize in the cubic CsCl structure. However, they possess very different mass ratios, i.e., 5.76 and 2.56 for TlCl and TlBr, respectively. Both TlCl and TlBr are not strictly ionic and exhibit partial covalency due to the presence of d-electrons in their cations [3]. No high-pressure thermal conductivity data exist for TlCl and TlBr. The present study was undertaken in an attempt to

[1] National Institute for Materials Research, Council for Scientific and Industrial Research, P.O. Box 395, Pretoria 001, Republic of South Africa.

0195-928X/87/0900-0607$05.00/0

determine the major mechanisms of heat conduction in these materials and the influence of the mass ratio on these mechanisms and to test the degree to which the results can be correlated with the trends observed in the alkali halides.

2. EXPERIMENTAL

The transient hot-wire method as described in Refs. 4 and 5 was used to measure the thermal conductivity, λ.

Figure 1 shows the design of the high-pressure capsule used in the experiments. The assembled cell was located in the bore of a 30-mm pressure vessel and a piston driven by the hydraulic ram of a 3000-kN Kennedy press was used to generated the load. The diameter of the sample stack was 22 mm and it was located between two concentric cylinders of fired pyrophyllite. The temperature was controlled by cooling the massive pressure vessel by a controlled flow of liquid nitrogen and was determined from the measured change in resistance of the Ni wire. This capsule can operate up to 700 K. Because of the high toxicity of TlCl and TlBr, no data

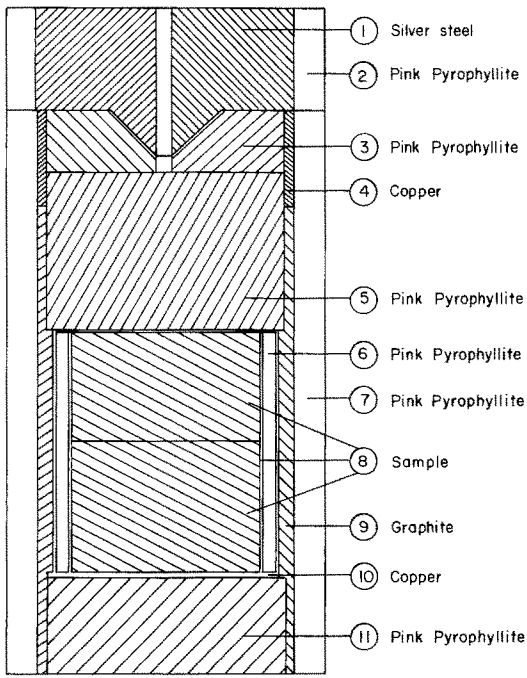

Fig. 1. Schematic diagram of the high-pressure capsule.

were obtained at high temperatures during these experiments. The resistivity of the particular Ni wire batch used had been determined very accurately as a function of temperature during previous experiments.

The hot wire was sandwiched between two precompacted plates of the sample material. The wire used had a diameter of 0.127 mm and was installed in a circular loop on the sample surface. Four leads were spot-welded to the wire to allow four-point resistance measurements to be performed. Any distortion of the wire under pressure was calculated from the measured electrical resistance of the wire, as described by Andersson and Bäckström [5].

In these experiments a computer-controlled data acquisition system was used to generate and record the thermograms. An HP 9816 desktop computer coupled to two high-sensitivity digital voltmeters, a control unit, and a disc drive formed the measurement system.

The nickel hot wire was connected in series with a standard resistor, R_s, a 45-Ω resistor, and a constant-voltage power supply as shown in Fig. 2. The voltages across the Ni wire and the standard R_s were monitored simultaneously every 27 ms by two high-sensitivity (5.5-digit) voltmeters. At the onset of a measurement, a negligible current of $\sim$1 mA flowed in the circuit. This enabled the ambient temperature of the sample to be evaluated prior to the application of the heating current. After 0.5 s, an electronic switch across the 45-Ω resistor was closed, effectively increasing the current to 2 A. Data were recorded for 1 s.

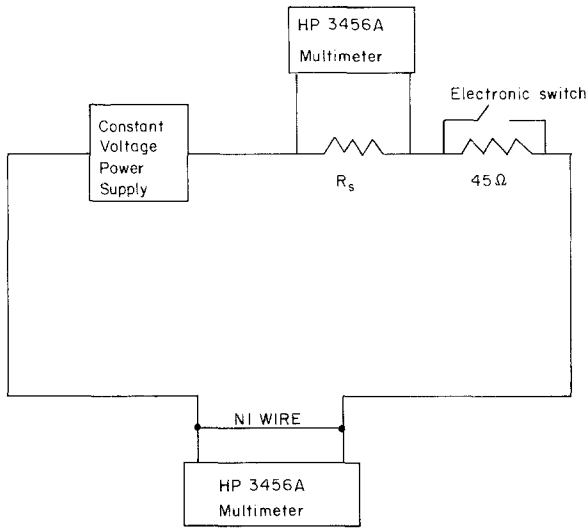

Fig. 2. Schematic diagram of the data acquisition system.

The voltages across the R_s and the Ni wire were used to calculate the resistance of the Ni wire as a function of time. Using the resistance vs temperature calibration a temperature–time profile was evaluated.

The value of the standard resistor was chosen to match that of the Ni wire as closely as possible. This ensured that the constant-voltage power supply delivered constant power across the Ni wire for the duration of the measurement.

Figure 3 shows a typical plot of temperature versus $\ln(t)$. A linear regression fit was made to the experimental points and hence the thermal conductivity was determined, as described in Ref. 5. The entire measurement cycle, including the determination of λ, required 2 min.

The material used in the experiments was powder (>99.5% purity) obtained from Merck, West Germany. It was compacted in a steel die to 0.3 GPa to form polycrystalline plates 22 mm in diameter and 12 mm thick. The capsule was dried in a vacuum oven prior to its being mounted in the press.

For each sample, three isobars were recorded, one at 0.5, one at 1, and one at 2 GPa, over the temperature range of 120–300 K. In addition, an isotherm from 0 to 2.3 GPa was measured at ambient temperature for each material.

3. RESULTS

The experimental results of the present work are shown in Figs. 4 to 7. Figure 4 shows a plot of thermal conductivity versus pressure for TlCl and TlBr. Three thermograms were recorded at each pressure and the scatter in

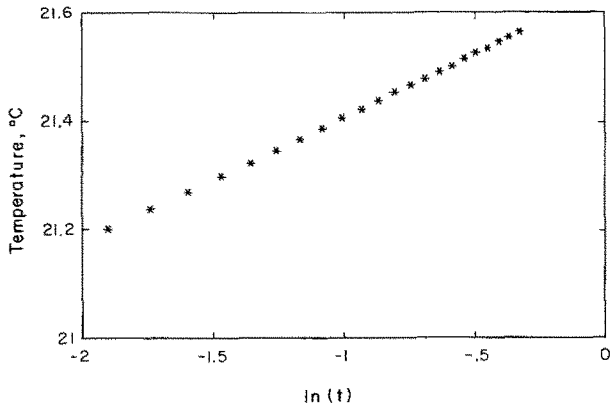

Fig. 3. Nickel wire temperature vs $\ln(t)$, where time, t, is in seconds.

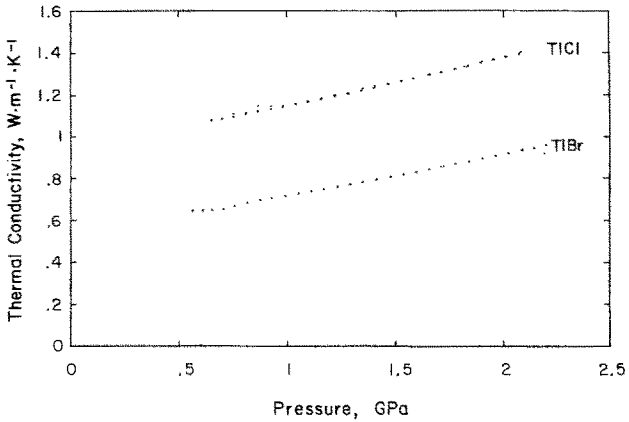

Fig. 4. Thermal conductivity of TlCl and TlBr as a function of pressure.

the data was negligible. A regression fit was made to the experimental data and the results are shown in Table I. In Fig. 5 the measured thermal resistivity $W = 1/\lambda$ as a function of temperature is plotted for TlCl at three isobars. Each line comprises many data points recorded with the data acquisition system. The solid line is a linear-regression fit to the experimental data extrapolated to zero pressure.

Our results at zero pressure may be compared with those of previous investigators. Agreement is within 10% in the case of both Giacomini [6] and McCarthy and Ballard [7].

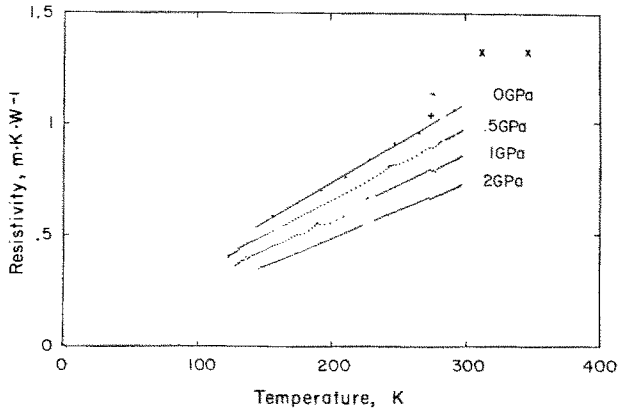

Fig. 5. Thermal resistivity of TlCl as a function of temperature. (+) Giacomini [6]; (×) McCarthy and Ballard [7].

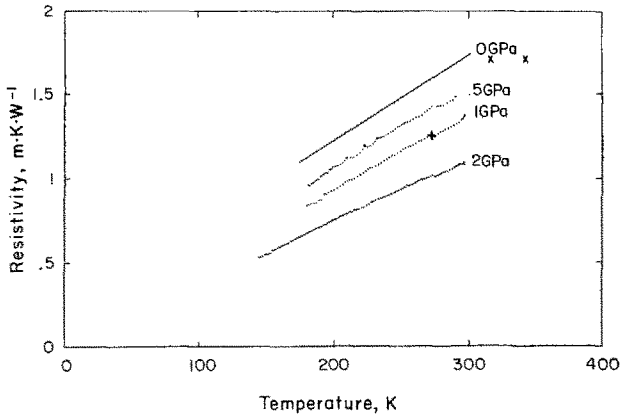

Fig. 6. Thermal resistivity of TlBr as a function of temperature. (+) Giacomini [6]; (×) McCarthy and Ballard [7].

Figure 6 shows thermal resistivity versus temperature data for TlBr. As before, three isobars were recorded and the solid line is a linear regression fit to the data extrapolated to zero pressure. Agreement with the ambient pressure data of McCarthy and Ballard [7] is within 5%, while the value of Giacomini [6] is about 20% lower than our experimental value at zero pressure.

The temperature dependence of the thermal conductivity of TlBr and TlCl has been measured recently by Suemune [8] at ambient pressure. He reports the occurrence of an anomalous minimum in thermal conductivity

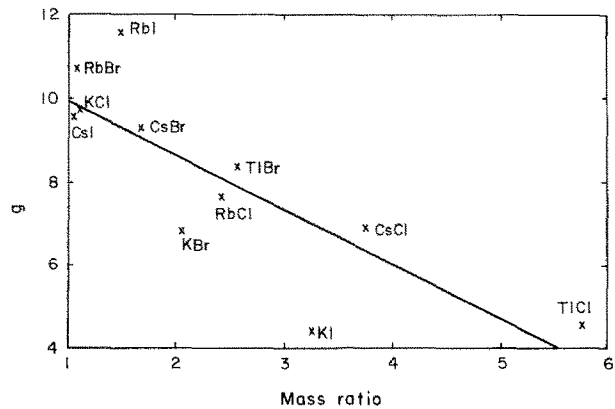

Fig. 7. g value (at zero pressure) versus mass ratio for compounds in the CsCl crystal structure.

Table I. Thermal Conductivity Versus Pressure at Ambient Temperature Fitted to Equations of the Form $\lambda = A + BP + CP^2$

Material	A ($W \cdot m^{-1} \cdot K^{-1}$)	B ($W \cdot m^{-1} \cdot K^{-1} \cdot GPa^{-1}$)	C ($W \cdot m^{-1} \cdot K^{-1} \cdot GPa^{-2}$)
TlCl	0.950	0.183	0.016
TlBr	0.523	0.194	0.

near 200 K for both materials. No such minima were observed in our experiments. In addition, the absolute values of thermal conductivity obtained by Suemune at 300 K were more than three times greater than our measured values in both cases.

Lawless [9] has measured the thermal conductivity of TlBr and TlCl in the low-temperature range 1.7–20 K at ambient pressure. Extrapolation of his results to the lowest temperatures measured in our experiments yields agreement within 6% for TlBr and within 12% for TlCl.

Linear regression fits were made to the W vs T curves and the results are shown in Table II.

4. DISCUSSION

4.1. Absolute Value of Thermal Conductivity

The high-temperature thermal conductivity of insulators is usually described by the Leibfried–Schlömann formula. According to the Leibfried–Schlömann theory λ is given by [10]

$$\lambda = Bn^{1/3}\, \delta \bar{M} \theta_\infty^3 \gamma_\infty^{-2} T^{-1} \tag{1}$$

Table II. Isobaric Temperature Dependence of W Fitted to Equations of the Form $W = A + BT$

Material	Pressure (GPa)	A ($m \cdot K \cdot W^{-1}$)	B ($m \cdot W^{-1}$)
TlBr	0	0.194	5.16×10^{-3}
TlBr	0.5	9.77×10^{-2}	4.85×10^{-3}
TlBr	1	3.32×10^{-2}	4.50×10^{-3}
TlBr	2	1.61×10^{-3}	3.72×10^{-3}
TlCl	0	3.21×10^{-2}	3.68×10^{-3}
TlCl	0.5	1.14×10^{-2}	3.25×10^{-3}
TlCl	1	8.94×10^{-3}	3.26×10^{-3}
TlCl	2	-0.299×10^{-2}	2.91×10^{-3}

where $\bar{M}$ is the average atomic weight, δ^3 is the average volume per atom, n is the number of atoms per primitive unit cell, and θ_∞ and γ_∞ are the Debye temperature and Grüneisen parameter, respectively. The value of the constant B is assume to be $3.04 \times 10^4\ \mathrm{W \cdot m^{-2} \cdot K^{-3}}$ [10]. This expression is valid if one may assume that only acoustic phonons contribute to the thermal conductivity via three phonon processes.

If only acoustic phonons contribute to the thermal properties, then θ_∞ and γ_∞ become $\bar{\theta}_\infty$ and $\bar{\gamma}_\infty$ where the parameters are evaluated over the acoustic phonon spectrum. If optic phonons also make a contribution to λ, then the values of the Debye temperature and Grüneisen parameter should be those calculated over the whole spectrum, i.e., θ_∞ and γ_∞.

The values of $\bar{\theta}_\infty$ and θ_∞ were calculated by integrating over the phonon density of states of TlCl and TlBr, as determined from neutron scattering experiments [11]. The Grüneisen parameter was taken to be equal to the room-temperature thermodynamic Grüneisen parameter

$$\gamma\ (\text{thermodynamic}) = \frac{3\alpha B_s}{\rho C_p}$$

where B_s is the adiabatic bulk modulus, α is the linear thermal expansion coefficient, ρ is the density, and C_p is the specific heat at constant pressure, as given by Redmond and Yates [12].

In Table III, the values of λ at 293 K, calculated using Eq. (1), are shown for the two cases of acoustic photons or all phonons taking part in the heat transport. The values of the input parameters used in the calculations are included as well as the measured values of λ for comparison.

From Table III, it can be seen that the measured value of λ lies between the two calculated values at 293 K. This suggests that in these materials the contribution of optic phonons to λ cannot be ignored.

4.2. Density Dependence of λ

Formal differentiation of λ with respect to density after Slack [10] gives

$$g = \left(\frac{\partial \ln \lambda}{\partial \ln \rho}\right)_T = B_T \left(\frac{\partial \ln \lambda}{\partial P}\right)_T \tag{2}$$

Table III. Calculated and Measured Values of the Thermal Conductivity of TlCl and TlBr at Zero Pressure and 293 K

Material	T (K)	$\bar{M}$ (g-atom)	δ (10^{-10})	θ_∞ (K)	$\bar{\theta}_\infty$ (K)	γ	$\bar{\lambda}_{\text{calc}}$ ($\mathrm{W \cdot m^{-1} \cdot K^{-1}}$)	λ_{calc} ($\mathrm{W \cdot m^{-1} \cdot K^{-1}}$)	λ_{meas} ($\mathrm{W \cdot m^{-1} \cdot K^{-1}}$)
TlCl	293	119.91	2.63	168	84	2.47	0.318	2.543	0.95
TlBr	293	142.14	2.73	112	65	2.41	0.190	0.974	0.52

This can be written as

$$g = 3\gamma + 2q - \frac{1}{3} \tag{3}$$

$$\gamma = \left(\frac{\partial \ln \theta}{\partial \ln \rho}\right)_T = B_T \left(\frac{\partial \ln \theta}{\partial P}\right)_T$$

and

$$q = -\left(\frac{\partial \ln \gamma}{\partial \ln \rho}\right)_T = -B_T \left(\frac{\partial \ln \gamma}{\partial P}\right)_T$$

where B_T is the isothermal bulk modulus.

The parameter q is the second Grüneisen parameter. Table IV shows the values of g calculated from Eq. (3) for zero pressure, compared with experimental values calculated from Eq. (2). The values of γ used are once again the room-temperature thermodynamic Grüneisen parameters. The q values are calculated from the third-order elastic constant data by the method of Rao [13]. The adiabatic bulk modulus B_s, required for Rao's method was calculated from the equation $B_s = \frac{1}{3}(C_{11} + 2C_{12})$. $B_T = B_s(1 + 3\alpha\gamma T)^{-1}$ could then be used in Eq. (2) to obtain the experimental value of g. Values of the elastic constants and their pressure derivatives for both compounds were obtained from Landolt-Börnstein [14]. The agreement with experiment, particularly for TlCl, is very poor. Similar poor agreement has been observed in the case of the B2 phase of the potassium and rubidium halides by Slack and Ross [2]. Figure 7 shows the zero-pressure g values of the CsCl-structure alkali halides plotted as a function of the mass ratio. The g values for the high-pressure phases of the potassium and rubidium halides were calculated from the λ versus P data of Andersson [15], extrapolated to zero pressure, and the V/V_0 data of Vaidya and Kennedy [16]. The cesium halide g values were taken from

Table IV. Values of g Calculated from $3\gamma + 2q - \frac{1}{3}$, Compared with Those Obtained by Experiment

				0 GPa		2 GPa	
Material	γ	q	B_s (GPa)	g_{obs}	g_{calc}	g_{obs}	g_{calc}
TlCl	2.47	3.9	23.6	4.07	14.88	6.0	13.2
TlBr	2.41	3.2	22.2	7.56	13.30	7.0	11.8

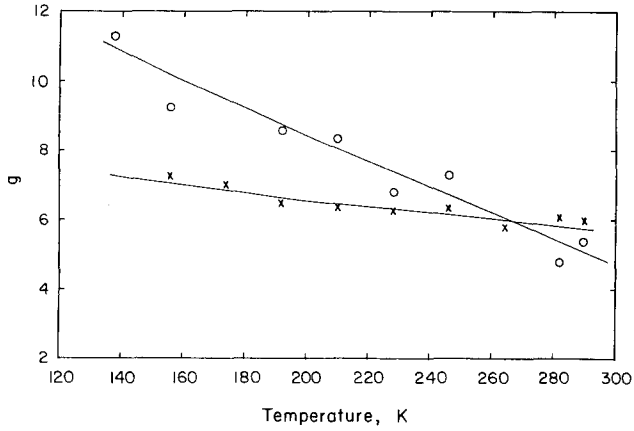

Fig. 8. g value versus temperature for TlCl and TlBr. (×) TlCl; (○) TlBr.

the data of Gerlich and Andersson [17]. The graph shows a decreasing value of g with increasing mass ratio, in contrast with the NaCl-structure alkali halides, where the opposite trend has been observed [2].

Figure 8 shows the variation of g value with temperature for the two materials. These values were obtained from the experimental data in Figs. 5 and 6, via Eq. (2). The temperature dependence of B_T was obtained from Landolt-Börnstein [14]. The value for TlCl varies very little, while the value for T1Br decreases with increasing temperature.

Figure 9 shows the pressure variation of g as obtained from the experimental results in Fig. 4 and Eq. (2). The value of the bulk modulus

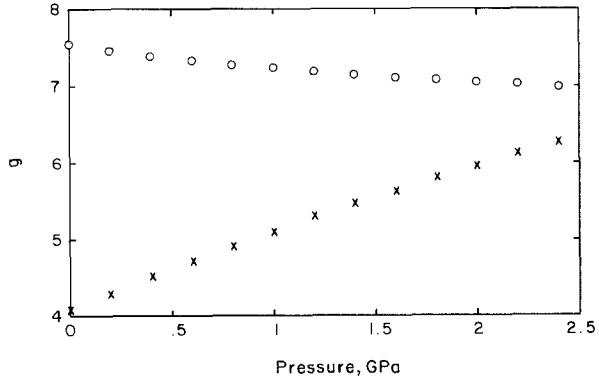

Fig. 9. g value versus pressure for TlCl and TlBr. (×) TlCl; (○) TlBr.

and its pressure dependence was obtained from Landolt–Börnstein [14]. The value for TlBr shows a decrease with increasing pressure, while the value for TlCl increases slightly.

The volume dependence of g can be expressed as $g = 3\gamma_0(V/V_0)^q + 2q - \frac{1}{3}$, where γ_0 is the Grüneisen parameter at zero pressure and V/V_0 is the relative volume at pressure P. We used the values of γ and q as given in Table IV. The values of V/V_0 were obtained from elastic constant data [14], with the aid of a first-order Murnaghan equation. The pressure dependence of the unit volume of TlCl was also measured in our own laboratory, using a volumetric technique, described in Ref. 18. The data were found to be in agreement with the predictions of the Murnaghan equation to within 0.5%. Table IV shows the values of g thus calculated for the two materials at 2 GPa. The experimentally determined values are shown for comparison. It is interesting to note that the theoretical prediction shows g to decrease with pressure for both compounds, while experiment shows that this is not the case for TlCl. In view of the approximations in the theoretical estimate, it is not possible to assess the significance of this discrepancy at present.

4.3. Isochoric Temperature Dependence of $W(=1/\lambda)$

If Eq. (1) is valid we would expect the thermal resistivity to be proportional to T. This equation is strictly valid only under isochoric conditions.

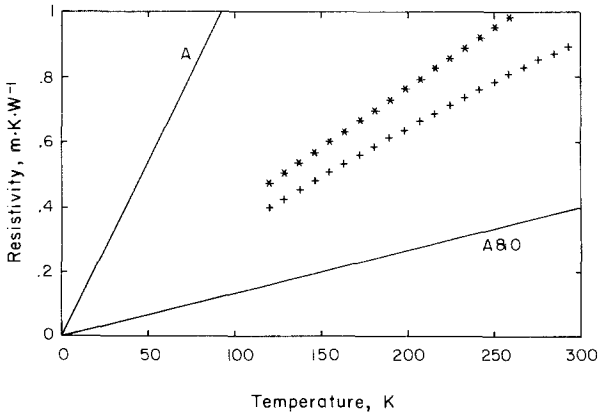

Fig. 10. Thermal resistivity as a function of temperature for TlCl. (+) Isochoric data for volume at $P = T = 0$. (*) Isobaric data for $P = 0$. The solid lines represent Eq. (1) in the two cases of acoustic phonons (A) and acoustic and optic phonons (A & O) taking part in the heat transport.

Since the value of g as a function of temperature has been determined, we may reduce our isobaric data to isochoric conditions. The volume at $P=0$ and $T=0$ was chosen. For the reduction we used $W(T)$ at zero pressure from Table II, $g(T)$ (Fig. 8), and $\alpha(T)$ given by Redmond and Yates [12]. The results are shown in Figs. 10 and 11. In both cases the isochoric data shows a downward curvature at high temperature. It has been predicted by Auerbach and Allen [19], based on the observed strong T-dependent phonon broadening in these materials, that TlCl and TlBr should exhibit saturation effects in λ at 300 K and above. The observed flattening off in the W vs T curves in these materials may therefore be attributable to the onset of saturation.

The fact that the TlBr curve does not extrapolate through the origin is contrary to the prediction of the Leibfried–Schlömann formula.

Although a straighforward Leibfried–Schlömann-type analysis does not seem to be applicable to these materials, it is significant that the experimental values lie between the two solid lines representing the theoretical predictions for the thermal resistivity when heat is transported by acoustic phonons only or by all phonons. This confirms our earlier suggestion that both optic and acoustic phonon contributions need to be taken into account for these materials. In fact, the proximity of the isochoric curves to the "acoustic and optic" straight lines would indicate

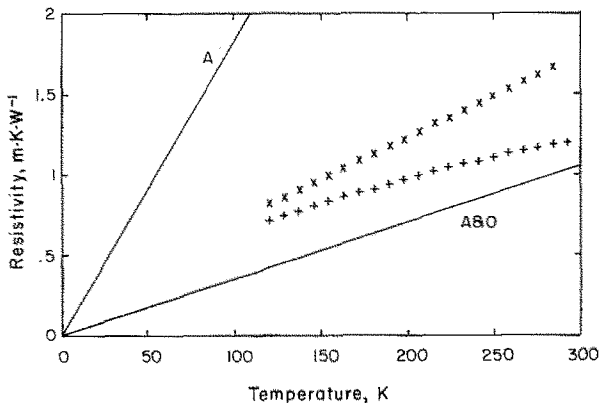

Fig. 11. Thermal resistivity as a function of temperature for TlBr. (+) Isochoric data for volume at $P=T=0$. (×) Isobaric data for $P=0$. The solid lines represent Eq. (1) in the two cases of acoustic photons (A) and acoustic and optic phonons (A & O) taking part in the heat transport.

Table V. Coefficients for Isochoric Thermal Conductivity Fitted to Equations of the Form $\lambda = A + BT^x$

Material	A ($W \cdot m^{-1} \cdot K^{-1}$)	B ($W \cdot m^{-1} \cdot K^{-(1+x)}$)	x
TlCl	0.297	455.01	−1.1125
TlBr	0.271	51.272	−0.795

that the optic modes play a rather important role in the heat transport process in these materials.

4.4. Correction for Minimum Conductivity

Since the Debye temperatures of TlBr and TlCl are low, correction of the data for the effect of minimum thermal conductivity may be expected to be significant [20]. The isochoric data for TlCl and TlBr were fitted empirically to equations of the form $\lambda = A + BT^x$, A being the value of the minimum thermal conductivity. The results obtained are shown in Table V.

Since the minimum thermal conductivity is essentially independent of pressure, it may be subtracted from the measured value of λ at zero pressure, λ_0, and the resulting value, $\lambda_0 - \lambda_\infty$, may be used to calculate a corrected g value which will not contain the nonpropagating photon part. The results are shown in Table VI. The corrected g values are higher than those given in Table IV, thus giving a better agreement with the prediction for g as derived from the Leibfried–Schlömann formula. This is particularly pronounced in the case of TlBr. This ought to be expected, as the Debye temperature of this material is lower than that of TlCl.

5. CONCLUSIONS

It appears that the Leibfried–Schlömann formula cannot describe the thermal conductivity of TlBr and TlCl very satisfactorily. In both these

Table VI. Values of the Minimum Thermal Conductivity, λ_∞, and g Values Corrected for the Effect of λ_∞

Material	λ_∞ ($W \cdot m^{-1} \cdot K^{-1}$)	g (corrected)
TlCl	0.297	6.14
TlBr	0.271	15.4

compounds the optic phonon modes appear to make a significant contribution to the heat transport. The use of the minimum thermal conductivity of these materials leads to better agreement between experiment and the Leibfried–Schlömann theory. More theoretical work is necessary before the thermophysical properties of these materials are properly understood.

ACKNOWLEDGMENTS

It is a pleasure to acknowledge Dr. G. A. Slack's helpful remarks on a preliminary draft of this paper. We are also grateful to Mr. J. G. Auret for measuring the pressure dependence of the volume of TlCl.

REFERENCES

1. R. G. Ross, P. Andersson, and B. Sundquist, *Rep. Prog. Phys.* **47**:1347 (1984).
2. G. A. Slack and R. G. Ross, *J. Phys. C Solid State Phys.* **18**:3957 (1985).
3. R. K. Singh and P. Khare, *J. Phys. Soc. Jap.* **51**:141 (1982).
4. R. G. Ross, P. Andersson, and G. Bäckström, *Mol. Phys.* **38**:377 (1979).
5. P. Andersson and G. Bäckström, *Rev. Sci. Instrum.* **47**:205 (1976).
6. Giacomini, *Int. Crit. Tables* **5**:231 (1929).
7. K. A. McCarthy and S. S. Ballard, *J. Opt. Soc. Am.* **41**:1062 (1951).
8. Y. Suemune, *Phys. Soc. Jap.* **52**:2816 (1983).
9. W. N. Lawless, *Phys. Rev.* **B30**:6057 (1984).
10. G. A. Slack, *Solid State Physics, Vol. 34*, F. Seitz, D. Turnbull, and H. Ehrereich, eds. (Academic Press, New York, 1979), pp. 1–71.
11. M. S. Kushwaha, *Physica* **125B**:45 (1984).
12. A. D. Redmond and B. Yates, *J. Phys. C Solid State Phys.* **5**:1589 (1972).
13. R. R. Rao, *J. Phys. Soc. Jpn.* **38**:1080 (1975).
14. Landolt-Börnstein, *Numerical Data and Functional Relationships in Science and Technology, Vol. 11* (Springer Verlag, New York, 1979), p. 30, 89, 106.
15. P. Andersson, *J. Phys. C Solid State Phys.* **18**:3943 (1985).
16. S. N. Vaidya and G. C. Kennedy, *J. Phys. Chem. Solids* **32**:951 (1971).
17. D. Gerlich and P. Andersson, *J. Phys. C Solid State Phys.* **15**:5211 (1982).
18. I. Sigalas, J. G. Auret, and S. Hart, *S. Afr. J. Phys.* **8**:83 (1985).
19. A. Auerbach and P. B. Allen, *Phys. Rev. B* **29**:2884 (1984).
20. G. A. Slack, *Phys. Rev. B* **26**:1873 (1982).